River Flow 2010 - Dittrich, Koll, Aberle & Geisenhainer (eds) - © 2010 Bundesanstalt für Wasserbau ISBN 978-3-939230-00-7

An accurate well-balanced, generalized Roe-type approach for the simulation of debris flows over mobile bed

G. Rosatti & L. Begnudelli
CUDAM - Centro Universitario per la Difesa Idrogeologica dell'Ambiente Montano, Dipartimento di Ingegneria Civile ed Ambientale; via Mesiano, 77 I-38123 Povo (TN), Italy

ABSTRACT: this work presents an accurate Riemann Solver for the two-phase, mobile-bed debris-flow equations. The solver is characterized by the capability of including the nonconservative term in the developement of the Riemann-problem solution leading to a well-balanced approach. The proposed scheme has been implemented in a new version of the TRENT-2D code, a depth-integrated two-phase debris-flow model developed by one of the authors. The noteworthy increase of the model accuracy, due to the significant reduction in the numerical diffusion, will be presented by comparing the results of the two versions of the model when applied to test cases and real cases as well. The analysis of some unphysical discontinuous steady solutions admitted by the original equation system highlight the necessity to account for some important physical mechanisms such the influence of the bed slope on the direction of the sediments. This feature has been included in an approximated way in the model and its influence on the simulation is illustrated.

Keywords: Debris-flow, Mobile-bed, Two-phase flow, Generalized Roe Solver, Well-balance

1 INTRODUCTION

Two-dimensional numerical simulation of debris-flow is becoming a key instrument not only for back analysis but also for forecasting analysis, i.e. for hazard mapping. It is therefore important to keep on developing models with increased capacity to describe real events.

In the Alpine regions, debris flows are very often characterized by a two-phase behaviour with a rheology that is essentially grain-inertial (Armanini et al., 2009). Therefore much of the research effort is devoted to this type of flow. The relevant system of equations can be obtained from the mass and momentum conservation of each phase. Several simplifications are generally accepted as good approximations for most of the flow conditions that occur in actual real debris-flow events (see sect. 2) and the shallow-water assumptions are applied in order to obtain two-dimensional models.

From a numerical point of view, the system of partial differential equations presents challenging problems connected to its intrinsic non-conservative nature and to the strong nonlinearity of the relations between primitive and conserved variables.

In this paper we present the result of our effort to improve the capabilities of the TRENT2D model (acronym for Transport in Rapidly Evolutive, Natural Torrent, see Armanini et al., 2009). In particular we present a new numerical scheme that appears to be much less diffusive respect the original one employed in the TRENT2D model. This scheme is based on a generalized Roe-type approach that allows dealing with the non conservative term of the equation in the solution of a Riemann problem that develops on the sides of the cells in a Godunov numerical framework. Moreover, this scheme is intrinsically well-balanced (i.e. it solves exactly the steady-state solutions) because it is based on exact Rankine-Hugoniot relations.

The other novelty introduced in this paper is the introduction of a “diffusive” terms in the system. In fact, the original system, allows some steady discontinuous solutions that are not physically acceptable. This is essentially due to the fact that the original system neglects some mechanisms that can play a fundamental role in some two-dimensional situations. For instance, depth-

averaged sediment velocity may deviate from the averaged fluid velocity because of the transversal slope of the bed. This mechanism, well known in classical sediment transport, is not yet observed in debris flows and its actual existence must be supported by suitable experimental evidence. Other mechanisms that actually occur in mobile-bed situations are bed sliding, bank failure and so on. In this work, we have propose an approach for including all of these mechanisms, all lumped in one extra term.

The paper is structured as follows: section 2 presents the mathematical model while in section 3 the numerical strategy is outlined. In sec. 4 we present the comparison between the new approach and the old one. Conclusions end the paper.

2 THE MATHEMATICAL MODEL

The mathematical model is a free-surface, mobile-bed, depth-integrated, shallow-water two-phase flow in which the solid and the liquid fraction interact each other and with the bed. The mathematical system is constituted by the conservation equation of solid mass, mixture mass and mixture momentum in which the following assumptions are then introduced: interphase forces due to possible slight deviations between velocities of the solid and liquid phases are negligible; the pressure distribution are linear along the vertical direction; the concentration is constant through the flow depth; the tangential stresses act only along the bed. More detail on the equations and the assumptions can be found in Armanini et al. (2009).

The resulting model is described by the following system:

$$\frac{\partial \mathbf{U}}{\partial t}+\frac{\partial \mathbf{F}}{\partial x}+\frac{\partial \mathbf{G}}{\partial y}+\mathbf{H}_x\frac{\partial \mathbf{W}}{\partial x}+\mathbf{H}_y\frac{\partial \mathbf{W}}{\partial y}=\mathbf{T}_x+\mathbf{T}_y \quad (1)$$

where the vector of conserved variable **U** and the conservative fluxes **F** and **G** are defined as:

$$\mathbf{U}=\begin{bmatrix} h+z_b \\ ch+c_b z_b \\ c^{\delta}\,uh \\ c^{\delta}\,vh \end{bmatrix} \quad (2)$$

$$\mathbf{F}=\begin{bmatrix} uh \\ cuh \\ c^{\delta}\left(u^2h+\frac{gh^2}{2}\right) \\ c^{\delta}\,uvh \end{bmatrix};\quad \mathbf{G}=\begin{bmatrix} vh \\ cvh \\ c^{\delta}\,uvh \\ c^{\delta}\left(v^2h+\frac{gh^2}{2}\right) \end{bmatrix} \quad (3)$$

where h is the mixture depth, z_b is the bed elevation above a reference horizontal plane, c is the mixture concentration, c_b is the sediment concentration in the bed (assumed constant), u and v are the x and y components of the depth-averaged mixture velocity and $c^{\delta}=(1+c\Delta)$, where $\Delta=(\rho_s-\rho_w)/\rho_w$, being ρ_s and ρ_w the densities of the liquid and solid phase respectively. $\mathbf{H}_x\partial\mathbf{W}/\partial x$ and $\mathbf{H}_y\partial\mathbf{W}/\partial y$ are the non conservative terms deriving from the pressure exerted by the bed on the control volume, where $\mathbf{W}=(h,\ z_b,\ u,\ v)^{\mathrm{T}}$ is the vector of the primitive variables and

$$\mathbf{H}_x=\begin{bmatrix} 0&0&0&0\\ 0&0&0&0\\ 0&0&0&\Gamma\\ 0&0&0&0 \end{bmatrix};\quad \mathbf{H}_y=\begin{bmatrix} 0&0&0&0\\ 0&0&0&0\\ 0&0&0&0\\ 0&0&0&\Gamma \end{bmatrix} \quad (4)$$

where $\Gamma=c^{\delta}gh$ and g is the gravitational acceleration. Finally,

$$\mathbf{T}_x=\begin{bmatrix} 0\\ 0\\ -\tau_x/\rho_w\\ 0 \end{bmatrix};\quad \mathbf{T}_y=\begin{bmatrix} 0\\ 0\\ 0\\ -\tau_y/\rho_w \end{bmatrix} \quad (5)$$

where $\boldsymbol{\tau}_b=(\tau_x,\tau_y)$ are the x and y component of the bed tangential stress vector.

In order to close the problem, some relationships must be introduced. Regarding the tangential stress $\boldsymbol{\tau}_b$, we used Bagnold's relation integrated on the depth and modified by Takahashi (1978) on the basis of experimental data. Assuming that there is no phase-lag in module and direction between the depth-averaged velocity vectors of the solid and the liquid phases has been considered, Bagnold's scalar relation can be written in a vectorial framework as follows:

$$\boldsymbol{\tau}_b/\rho_w=F(\|\mathbf{u}\|,h)\,\mathbf{u} \quad (6)$$

with:

$$F(\|\mathbf{u}\|,h)=\frac{25}{4}\frac{\rho_s}{\rho_w}\sin\phi_d\,\frac{\lambda^2}{Y^2}\|\mathbf{u}\| \quad (7)$$

and

$$\lambda=\left[(c_b/c)^{1/3}-1\right]^{-1} \quad (8)$$

where ϕ_d is the dynamic friction angle of the material, $Y=h/da^{1/2}$ where d is the grain size, a is a constant that has been set to 0.042 by Bagnold and estimated equal to 0.32 by Takahashi (1978). In order to avoid numerical singularity when $h\to 0$ and to reduce the computational burden, we assumed Y as a characteristic parameter of the simulation, to be defined through a calibration process considering a series of experimental tests on the material of each simulated site.

As for the concentration c, we used the same relation that has been adopted in several works (Armanini 2009, Rosatti and Fraccarollo 2006, Rosatti et al. 2008), a closure relation that does not generate an excessive numerical burden but has a physically based structure. The adopted relation can be written in the following form:

$$c = c_b \beta \frac{\|\mathbf{u}\|^2}{gh} = \beta c_b \mathrm{Fr}^2 \tag{9}$$

Where β is a dimensionless transport parameter, estimated from laboratory data.

2.1 *Eigenstructure of the homogeneous system*

Considering the x-split homogeneous part of system (1) with the relevant closure relation (9), it presents four real and distinct eigenvalues where one of them is equal to the velocity in the y direction v. The connected fields are genuinely nonlinear (and therefore they can develop either rarefactions or shocks) for three eigenvalues while one is linearly degenerate for the field connected with $\lambda = v$. A symmetric result can be obtained for the y-split equations (with v in place of u).

2.2 *The generalized Rankine-Hougoniot relations*

The relations valid across a shock are not the standard Rankine-Hugoniot relations because the relevant system is not fully conservative. The role played by the non conservative term can be obtained by writing the momentum conservation principle in integral form applied to a mobile control volume with speed equal to the shock speed (see Fig. 1).

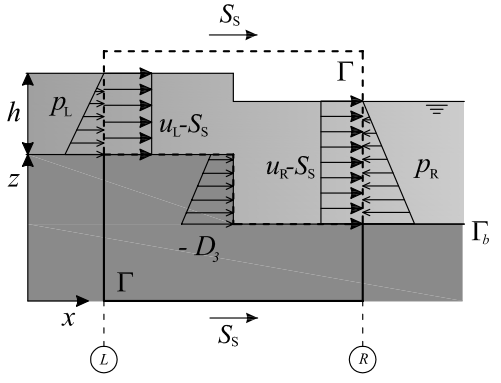

Figure 1. Sketch of the 1D control volume used to derive the Generalized Rankine Hugoniot equations.

The resulting relation, called Generalized Rankine-Hugoniot relation, present one more term respect the standard formulation (Rosatti and Fraccarollo, 2006):

$$\mathbf{F}_R - \mathbf{F}_L - \mathbf{D} = S_S(\mathbf{U}_R - \mathbf{U}_L) \tag{10}$$

where the **D** vector is non-null only for the momentum component. It represents the integral of the pressure exerted by the bed on the control volume. It is clear that the pressure distribution must depend on the actual flow behavior in the neighborhood and inside the bed discontinuity. Lacking experimental evidence some hypotheses must be introduced.

In this paper we will use the following relation, proposed in Rosatti and Fraccarollo (2006) (used also in Rosatti et al, 2008, Rosatti and Begnudelli, 2010) on the basis of physical considerations:

$$D = -g(1 + c_k \Delta)\left(h_k - \frac{|z_R - z_L|}{2}\right)(z_R - z_L)$$
$$\text{where} \quad k = \begin{cases} L & \text{if } z_L \le z_R \\ R & \text{otherwise} \end{cases} \tag{11}$$

It must be noticed that this relation derives from a "fixed-bed" approach, where the bed thrust is exactly equal to the fluid thrust. In case of mobile-bed, the pressure distribution may not be the same. For example the concentration should be equal to c_b and not c_k.

In any case, what is presented in the following sections is substantially independent on the assumed thrust relation.

2.3 *The necessity of a "diffusion" term*

Several effects, with diffusive behavior and that can play an important role in particular situations, are implicitly neglected in deriving system (1). For example if the bed is discontinuous or even if the slope is large, local sliding is likely to occur; moreover, sediments can diffuse from zone of higher concentration to zone of lower concentration; finally, the depth-averaged velocity vector of the solid phase may deviate from the depth-averaged vector of the liquid phase.

The necessity of a diffusion term capable, in some way, of overcoming the uncertainty of eq. (11) is suggested by a particular permanent solution of (1) that is rather unphysical. Let us consider a channel with initial cross section as in Fig. 2 with constant longitudinal slope S_0, null velocity in the y direction, depth and velocity equal to h_L and u_L in the left part of the channel (i.e., to the left of the bed discontinuity) and equal to h_R and u_R in the right part. In the y-direction, the steady solution satisfy the momentum balance, i.e. the shock condition (10) with $S_S = 0$, while in the x-direction uniform flows occur.

This particular solution is clearly unphysical because a steady discontinuity in the bed cannot exist in presence of a granular bed without cohesive features. This result suggests that relation (11) is not completely reliable. Moreover, in these

conditions the physical mechanism above mentioned may become important.

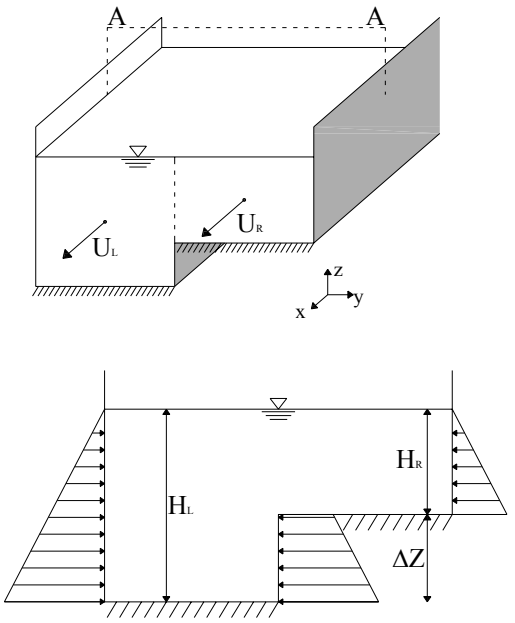

Figure 2. Sketch of the channel described in Section 2.3

In order to obtain more realistic results, we have faced the problem introducing a suitable term in the sediment continuity equation that summarizes, in some way, the combined effect of several processes as discussed before. In particular we consider the effect of the bed slope on the sediment velocity direction and we introduce in the model a term which is a function of $\nabla^2 z_b$.

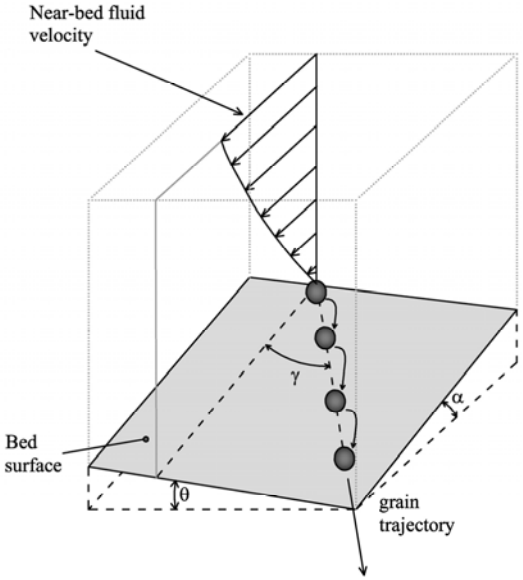

Figure 3. Fluid velocity, grain trajectories and generation of lateral bed load.

There are several theories that describe the effect of local bed slope (i.e., of gravity) on regular bed load transport (see e.g. Kovacs and Parker, 1994, Parker et al., 2003, Seminara et al., 2002). There is no theory available explicitly developed for the case of debris flow. However, it has been observed (Fraccarollo and Rosatti, 2009) that in the case of ordinary bed load, the concentration inside the transport layer reaches values typical of debris flow, and that, in absence of bed forms, there is clear analogy between the physics of bed load transport and of debris flows. Therefore, we simply considered the most widely accepted theories for the bed load and apply it to the case of debris flow introducing a calibration parameter that becomes a characteristic parameter of the simulation, to be defined through a calibration process considering a series of experimental tests on the material of each simulated site, just like Y.

In particular, we start from the lateral bed load formulation of Talmon et al. (1995). Considering a bed channel as in Figure 3, in which the near-bed fluid velocity is η and whose transverse direction is ξ, the deviation γ between the sediment transport direction and the flow direction can be written in the following form:

$$\tan\gamma = K\frac{\partial z_b}{\partial \xi} \tag{12}$$

Indicating the component of the sediment transport due to the bed slope with $q^{\nabla z}$, under the assumption that γ is small and thus $\tan\gamma \approx \sin\gamma$, we can write:

$$q^{\nabla z} \approx q\sin\gamma = Kq\frac{\partial z_b}{\partial \xi} \tag{13}$$

More in general, indicating with $\mathbf{q} = (q_x, q_y)$ the sediment transport discharge vector, the additional components $\mathbf{q}^{\nabla z} = (q_x^{\nabla z}, q_y^{\nabla z})$ due to the bed slope become:

$$\mathbf{q}^{\nabla z} = (q_x^{\nabla z}, q_y^{\nabla z}) = K\|\mathbf{q}\|\nabla z \tag{14}$$

By adding this sediment fluxes, Eq. (differential formulation) becomes:

$$\frac{\partial \mathbf{U}}{\partial t} + \frac{\partial \mathbf{F}}{\partial x} + \frac{\partial \mathbf{G}}{\partial y} + \mathbf{H}_x\frac{\partial \mathbf{W}}{\partial x} + \mathbf{H}_y\frac{\partial \mathbf{W}}{\partial y} = \mathbf{\Sigma} \tag{15}$$

where

$$\mathbf{\Sigma} = -\frac{\partial}{\partial x}\left(\mathbf{L}\frac{\partial \mathbf{W}}{\partial x}\right) - \frac{\partial}{\partial y}\left(\mathbf{L}\frac{\partial \mathbf{W}}{\partial y}\right) + \mathbf{T}_x + \mathbf{T}_y \tag{16}$$

and

$$\mathbf{L} = \begin{bmatrix} 0 & 0 & 0 & 0 \\ 0 & 0 & 0 & l \\ 0 & 0 & 0 & 0 \\ 0 & 0 & 0 & 0 \end{bmatrix} \tag{17}$$

where $l = K\|\mathbf{q}\|$.

3 THE NUMERICAL MODEL

The numerical method employed in the TRENT-2D model is described in Armanini et al. (2009). Here, we briefly recall the most important features and focus specifically on the flux evaluation, for which a new approach is proposed in this paper.

The scheme is based on a finite volume approach (on Cartesian meshes of rectangular cells)) and the update algorithm for the conserved variables is obtained by time integration on a interval Δt and spatial averaging on a cell area $A_{i,j}$ of system (15). A classical operator-splitting approach is adopted: firstly, the homogeneous part of eq. (15) is solved obtaining

$$\begin{aligned}\widetilde{\mathbf{U}}_{i,j}^{n+1} \;=\; & \mathbf{U}_{i,j}^{n} - \frac{\Delta t}{\Delta x}\left(\hat{\mathbf{F}}_{i+\frac{1}{2},j}^{n+\frac{1}{2}} - \hat{\mathbf{F}}_{i-\frac{1}{2},j}^{n+\frac{1}{2}}\right) \\ & - \frac{\Delta t}{\Delta y}\left(\hat{\mathbf{G}}_{i,j+\frac{1}{2}}^{n+\frac{1}{2}} - \hat{\mathbf{G}}_{i,j-\frac{1}{2}}^{n+\frac{1}{2}}\right) \\ & - \frac{\Delta t}{\Delta x}\Gamma_{i,j}^{n+\frac{1}{2}}\left(\mathbf{W}_{i+\frac{1}{2},j}^{n+\frac{1}{2}} - \mathbf{W}_{i-\frac{1}{2},j}^{n+\frac{1}{2}}\right) \\ & - \frac{\Delta t}{\Delta y}\Gamma_{i,j}^{n+\frac{1}{2}}\left(\mathbf{W}_{i,j+\frac{1}{2}}^{n+\frac{1}{2}} - \mathbf{W}_{i,j-\frac{1}{2}}^{n+\frac{1}{2}}\right)\end{aligned} \tag{18}$$

then the final solution is obtained by solving the ordinary differential equation (19) relative to source terms with the initial value $\widetilde{\mathbf{U}}_{i,j}^{n+1}$:

$$\frac{d\mathbf{U}}{dt} = \mathbf{\Sigma} \tag{19}$$

Following a MUSCL-Hancock explicit approach (Harten et al., 1983), quantities evaluated at time *n+1/2* in eq. (18) are obtained with a fully non conservative half-step after a linear reconstruction of the primitive variables. Side-cell fluxes $\hat{\mathbf{F}},\hat{\mathbf{G}}$ are evaluated from the solution of a local Riemann Problem (RP) generated by linear reconstruction of the primitive variable obtained in the previous half-step. The RP solution involves both conservative fluxes and the contribution of the pressure over the bed discontinuity (non conservative term). Details of the Riemann solver are given in the following section.

The resolution of equation (19) is made by Euler's implicit method in order to have no restrictions on the temporal step of integration:

$$\begin{aligned}\mathbf{U}_{i,j}^{n+1} = \widetilde{\mathbf{U}}_{i,j}^{n+1} + \Delta t\left[\left(\mathbf{T}_x\right)_{i,j}^{n+1} + \left(\mathbf{T}_y\right)_{i,j}^{n+1}\right] \\ - \frac{\Delta t}{\Delta y}\left(\left[l\frac{\partial \mathbf{W}}{\partial x}\right]_{i,j+\frac{1}{2}}^{n+1} - \left[l\frac{\partial \mathbf{W}}{\partial x}\right]_{i,j-\frac{1}{2}}^{n+1}\right) \\ - \frac{\Delta t}{\Delta x}\left(\left[l\frac{\partial \mathbf{W}}{\partial x}\right]_{i+\frac{1}{2},j}^{n+1} - \left[l\frac{\partial \mathbf{W}}{\partial x}\right]_{i-\frac{1}{2},j}^{n+1}\right)\end{aligned} \tag{20}$$

Finally, since the updating algorithm of the conserved variables copes simultaneously with both directions (unsplit approach), the following stability condition must be satisfied:

$$\frac{\Delta t}{\max[\Delta x,\Delta y]} < \frac{1}{2}\lambda_{\max} \tag{21}$$

where $\lambda_{\max}$ is the maximum eigenvalue associated to the homogeneous part of system (15), i.e. without $\mathbf{\Sigma}$.

3.1 *The Generalized Roe Solver*

The numerical fluxes $\hat{\mathbf{F}},\hat{\mathbf{G}}$ are obtained by using a Roe-type approach for the solution of the Riemann problem on each side of the cell. We report here the details for a RP in the *x*-direction; the values for the *y*-direction can be easily worked out with little effort.

The *x*-split RP is defined by the following non-conserative initial value problem:

$$\begin{cases}\dfrac{\partial \mathbf{U}}{\partial t} + \dfrac{\partial \mathbf{F}}{\partial x} + \mathbf{H}_x\dfrac{\partial \mathbf{W}}{\partial x} = 0 \\ \mathbf{U}(x,0) = \begin{cases}\mathbf{U}_L & \text{if } x<0 \\ \mathbf{U}_R & \text{if } x>0\end{cases}\end{cases} \tag{22}$$

The Generalized Roe Solver (Rosatti et. al., 2008) approximate (22) with the following linear RP:

$$\begin{cases}\dfrac{\partial \mathbf{U}}{\partial t} + \mathbf{J}_x(\mathbf{U}_L,\mathbf{U}_R)\dfrac{\partial \mathbf{U}}{\partial x} = 0 \\ \mathbf{U}(x,0) = \begin{cases}\mathbf{U}_L & \text{if } x<0 \\ \mathbf{U}_R & \text{if } x>0\end{cases}\end{cases} \tag{23}$$

where $\mathbf{J}_x(\mathbf{U}_L,\mathbf{U}_R)$ is a suitable matrix whose values depend on the left and right conditions. This matrix can be obtained by imposing the following conditions:

$$\mathbf{J}_x(\mathbf{U}_L,\mathbf{U}_R) = (\mathbf{A}' + \mathbf{A}'')\mathbf{B}^{-1} \tag{24}$$

where:

$$\mathbf{A}'_x(\mathbf{W}_R - \mathbf{W}_L) = \left(\mathbf{F}_R - \mathbf{F}_L\right) \tag{25}$$

$$\mathbf{A}''_x(\mathbf{W}_R - \mathbf{W}_L) = \mathbf{H}_x(\mathbf{W}_R - \mathbf{W}_L) \tag{26}$$

$$\mathbf{B}(\mathbf{W}_R - \mathbf{W}_L) = \mathbf{U}_R - \mathbf{U}_L \tag{27}$$

Matrices $\mathbf{A}'_x$ and $\mathbf{B}$ can be determined as Jacobian matrices respect to the primitive variables $\mathbf{W} = (h,u,v,z)$ evaluated for the following averaged values:

$$\tilde{h} = \frac{h_L + h_R}{2}$$
$$\tilde{u} = \frac{u_L\sqrt{h_L} + u_R\sqrt{h_R}}{\sqrt{h_L} + \sqrt{h_R}} \;\; ; \;\; \tilde{v} = \frac{v_L\sqrt{h_L} + v_R\sqrt{h_R}}{\sqrt{h_L} + \sqrt{h_R}} \quad (28)$$

Detailed expression of the components of these matrixes is not reported for lack of space while, all the coefficients of the matrix $\mathbf{A}_x^{"}$ are null except a_{34}'' whose value is

$$d = -g(1 + c_k\Delta)\left(h_k - \frac{|\delta_z|}{2}\right), K = \begin{cases} \text{L} & \text{if } z_L \le z_R \\ \text{R} & \text{otherwise} \end{cases} \quad (29)$$

Finally, the expression of the Generalized Roe numerical flux $\mathbf{F}^{\text{GR}}$ is:

$$\mathbf{F}^{GR} = \mathbf{F}_L + \sum_{m=1}^{4}(\lambda^- \mu\mathbf{R})^m = \mathbf{F}_R - \sum_{m=1}^{4}(\lambda^+ \mu\mathbf{R})^m \quad (30)$$

where

$$\begin{cases} \left(\lambda^+\right)^m = \left(1 + \text{sign}\left(\tilde{\lambda}^m\right)\right)\tilde{\lambda}^m \\ \left(\lambda^-\right)^m = \left(1 - \text{sign}\left(\tilde{\lambda}^m\right)\right)\tilde{\lambda}^m \end{cases} \quad (31)$$

$\tilde{\lambda}^m$ is the m-th eigenvalue of $\mathbf{J}_x(\mathbf{U}_L, \mathbf{U}_R)$ and $\mathbf{R}^m$ is the corresponding right eigenvector.

4 GENERALIZED ROE (GR) VS LHLL SCHEME

In this section we present the capabilities of the proposed GR method. Moreover, since we want to show the superiority of the proposed approach over the LHLL scheme used in the previous version of the TRENT2D model, we briefly present the features of the old one.

4.1 *The LHLL solver*

The momentum flux terms due to the bed discontinuities are modeled with the LHLL solver (first proposed by Fraccarollo et al., 2003) by considering two different values of the numerical flux on the left and right side of the face. For the x-direction

$$\mathbf{F}_{L,R}^{LHLL} = \mathbf{F}^{HLL} - \frac{S_{L,R}}{S_L - S_R}\tilde{\Gamma}\left(z_b^R - z_b^L\right) \quad (32)$$

where L, R are respectively the left and the right initial values of Riemann's problem, $\tilde{\Gamma} = \tilde{c}^{\delta} g\tilde{h}$ (where $\tilde{c}^{\delta} = (c_L^{\delta} + c_R^{\delta})/2$), F^{HLL} refers to an HLL (Harten et al., 1983) evaluation of the fluxes and

$$S_L = \min_{k=1,\ldots,3}\{\lambda_L^k, \lambda_R^k\} \;\; ; \;\; S_R = \max_{k=1,\ldots,3}\{\lambda_L^k, \lambda_R^k\} \quad (33)$$

being λ_L^k, λ_R^k with $k = 1,\ldots,3$ the 3 eigenvalues associated to the 1D version of system and evaluated with the values of the variables at the left (L) and right side (R) of the discontinuity.

This solver adds a corrective term to the expression given by the classical HLL approach that can be considered like a centered discretization of the term $(c\Delta + 1)gh\,\partial z_b/\partial x$ on the two sides of the face with weights $S_{L,R}/(S_L - S_R)$. Rosatti and Fraccarollo (2006) have demonstrated that such flux expression comes from approximating the solution of Riemann's problem with two shock-waves, as in the HLL scheme, supplemented by a central standing shock. In addition, this solution is based on the arbitrary assumption that there is no variation in the primitive variables $\mathbf{U}$ through the central shock.

4.2 *Accuracy and well-balanceness of the GR solver*

The accuracy of the GR solver has been already presented in the 1D case by Rosatti et al. (2008) where a comparison between computed and exact solutions have been shown. In the 2D case, exact solutions are available only in case of steady state conditions when the diffusive terms are neglected. In these cases, accuracy is connected with the well-balanceness of the scheme (i.e. the capability of reproduce steady solutions). Considering the solution presented in section 2.3, a possible solution is (with reference to Fig. 2): h_L = 1.711m, h_R = 0.711m ; u_R = 7.277m/s, u_L = 4.691m/s ; c_L = c_R = 0.107.

The result obtained by the code is equal to the exact solution and it is maintained in time indefinitely. This result is due to the fact (it can easily demonstrated) that the GR solver uses the exact generalized Rankine-Hugoniot relations in case of steady conditions. This result cannot be achieved with the LHLL scheme: starting from the same initial conditions, the solution smooth out in the y-direction because of its numerical diffusion. This behavior is due to the fact that LHLL uses only an approximation of the differential expression of the bed pressure and does not account in an accurate way the effect of the non conservative term in the solution of the RP.

4.3 *Estimate of the diffusion coefficient for the LHLL scheme*

Figure 4 shows the evolution of a cross section at time $t = 100$s using LHLL (thin solid line) and GR (bold solid line) solvers. As shown, the cross section undergoes important modifications using LHLL solver, while it does not vary at all using the Generalized Roe solver. This is actually the

correct solution, since the cross section should not vary in absence of lateral velocity and therefore lateral transport.

In fact, at $t = 0\,\mathrm{s}$ we have $v_y = 0$, and so it should be also for $t > 0\,\mathrm{s}$, since we have an exact momentum equilibrium across the bed discontinuity, and the governing equations do not contain diffusion terms in the sediment balance equation. Therefore, the evolution of the cross section given by the LHLL solver is entirely due to artificial numerical diffusion.

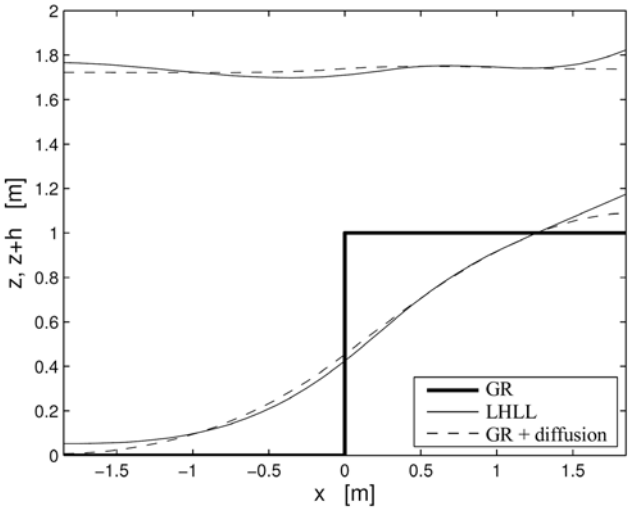

Figure 4. Evolution of a the cross section relative to the test case described in Sections 2.3 and 4.3 at time t = 100s.

Although the cross section obtained using the LHLL solver seems more realistic, the presence of such numerical diffusion is actually highly undesirable, because it is something we have no control upon. Thus, in order to model the diffusion processes that actually occur, it is more appropriate to use the GR solver and add a specific diffusion term rather that letting the numerical diffusion to mimic such process. In order to compare model predictions using the LHLL solver and GR solver plus the diffusion term, using the diffusion coefficient K (Eq. 16) as a calibration parameter. The best fitting (relative to the solutions at t = 100s) was achieved for $K = 7.6 \times 10^{-4}$. In Figure 4, the dashed lines represent the solution relative to the GR solver plus the diffusion term. In a practical case, the estimation should be based on laboratory experiment specifically tailored for type of process we want to simulate and for the type of terrain that constitute the bed. In fact, what we call "diffusion" also accounts for a variety of processes, like bed sliding, bank failure and so on. Actually, in this specific case, the real phenomenon involves geotechnical instability rather than diffusion, at least at an early stage, but there are cases where different mechanisms act together and it is extremely difficult to discern the effects of each process.

4.4 *Application to a realistic case*

Finally, we present the application of the numerical model to a realistic case, showing the differences between the results obtained by using the two solvers. The case we consider here regards a debris flow in a conoid situated in the Eastern Alps, near Trento.

Fig. 5 shows the predicted flow depths at a time just before the hydrograph peak that has been chosen as representative of the differences between

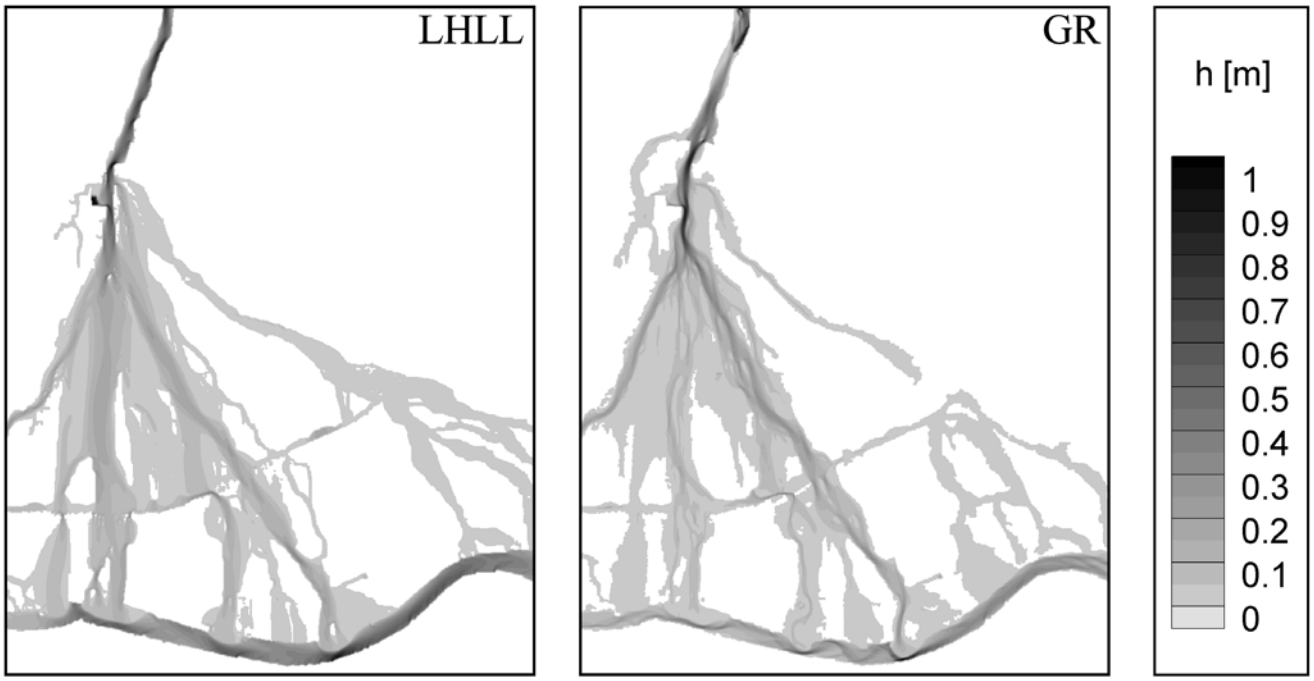

Figure 5. Application of the numerical model using LHLL solver (left) and GR solver without diffusion (right) to the simulation of a debris flow in a conoid situated in the Eastern Alps, near Trento.

the results obtained using the two solvers. The Generalized Roe solver has been used here without the diffusion term. There is of course no reference solution, so it is only possible to compare the two solutions and analyze the differences. As it can be seen, the two predictions are overall similar. There are though a few interesting differences, that can be easily connected with the numerical diffusion of the LHLL solver. The LHLL solution appears in fact everywhere smoother, and the discharge is more uniformly distributed. On the other hand, using the Generalized Roe solver, the flow is more concentrated in a few bigger streams, and the contour plot is overall more scattered. The same difference can be seen in the river (lower part of the pictures) that collects the water.

5 CONCLUSIONS

In this paper we have presented an improved version of the TRENT2D model for the simulation of debris flows over mobile bed. From the analysis of a possible steady solution of the conservation system we have realized that a diffusive term must added in the original system of conservation laws in order to obtain physically acceptable solutions. From a numerical point of view we have presented a new generalized Roe-type solver able to deal with non conservative fluxes present in the governing equations. This scheme is much less diffusive respect the original LHLL method because of the enhanced treatment of the non conservative term in the solution of the Riemann problem. This features allows to introduce proper discretization of diffusive terms (as well as possible other phenomena) without shadowing their effect because of the numerical diffusion of the scheme.

REFERENCES

Armanini A, Fraccarollo L, Rosatti G, 2009. Two-dimensional simulation of debris flows in erodible channels. Computers & Geosciences 35(5), 993-1006

Bagnold, R.A., 1954. Experiments on a gravity-free dispersion of large solid spheres in a Newtonian fluid under shear. Proceeding of the Royal Society. London A 225, 49-63.

Bernetti, R., Titarev, V.A., Toro, E.F. 2008. Exact solution of the Riemann problem for the shallow water equations with discontinuous bottom geometry, Journal of Computational Physics, 227, 3212-3243.

Fraccarollo, L., Capart, H., Zech, Y., 2003. A Godunov method for the computation of erosional shallow water transient. International Journal for Numerical Methods in Fluids, 41(9), 951-976.

Fraccarollo, L., Rosatti, G. 2009. Lateral bed load experiments in a flume with strong initial transversal slope, in sub- and supercritical conditions, Water Resour. Res, Vol. 45, W01419, doi:10.1029/2008WR007246.

Harten, A., Lax, P.D., Van Leer, B. 1983. On upstream differencing and Godunov-type schemes for hyperbolic conservation laws. SIAM Review, 61, 25-35.

Kovacs, A., Parker, G. 1994. A new vectorial bedload formulation andits application to the time evolution of straight river channels, J. Fluid Mech., 267, 153– 183.

Parker, G., Seminara, G., Solari, L. 2003. Bedload at low Shields stress on arbitrarily sloping beds: Alternative entrainment formulation, Water Resour. Res., 39(7), 1183, doi:10.1029/2001WR001253.

Rosatti, G., Fraccarollo, L. 2006. A well-balanced approach for flows over mobile-bed with high sediment-transport, Journal of Computational Physics, 220, 312-338.

Rosatti, G., Murillo, J., Fraccarollo, L. 2008. Generalized Roe schemes for 1D two-phase, free-surface flows over a mobile bed, Journal of Computational Physics, 227, 10058-10077.

Rosatti, G., Begnudelli, L. 2010. The Riemann problem for the one-dimensional shallow-water equations with a bed step: theoretical analysis and numerical simulations, Journal of Computational Physics, 229, 760–787

Seminara, G., L. Solari, and G. Parker (2002), Bedload at low Shields stress on arbitrarily sloping beds: Failure of the Bagnold hypothesis, Water Resour. Res., 38(11), 1249, doi:10.1029/2001WR000681.

Takahashi, T. 1978. Mechanical characteristics of debris flow, Journal of Hydraulic Division ASCE, 104(8), 1153-1169.

Talmon, A.M., Struiksma, N., van Mierlo, M.C.L.M. 1995. Laboratory measurements of the direction of sediment transport on trasverse alluvial-bed slopes, Journal of Hydraulic Research, 33(4), 495-517.